# Characterizing Small-Scale Dynamics of Navier-Stokes Turbulence with Transverse Lyapunov Exponents: A Data Assimilation Approach

Masanobu Inubushi,[1,2,*] Yoshitaka Saiki,[3] Miki U. Kobayashi,[4] and Susumu Goto[2]

[1]*Department of Applied Mathematics, Tokyo University of Science, Tokyo 162-8601, Japan*
[2]*Graduate School of Engineering Science, Osaka University, Osaka 560-8531, Japan*
[3]*Graduate School of Business Administration, Hitotsubashi University, Tokyo 186-8601, Japan*
[4]*Faculty of Economics, Rissho University, Tokyo 141-8602, Japan*

Data assimilation (DA) of turbulence, which involves reconstructing small-scale turbulent structures based on observational data from large-scale ones, is crucial not only for practical forecasting but also for gaining a deeper understanding of turbulent dynamics. We propose a theoretical framework for DA of turbulence based on the transverse Lyapunov exponents (TLEs) in synchronization theory. Through stability analysis using TLEs, we identify a critical length scale as a key condition for DA; turbulent dynamics smaller than this scale are synchronized with larger-scale turbulent dynamics. Furthermore, considering recent findings for the maximal Lyapunov exponent and its relation with the TLEs, we clarify the Reynolds number dependence of the critical length scale.

Predicting the future states of the Navier-Stokes (NS) turbulence is a huge challenge due to its chaotic dynamics over broad spatiotemporal scales. In general, observational data on small-scale turbulent structures are unavailable, yielding a small-scale initial-condition uncertainty. The small-scale uncertainty increases exponentially fast as $e^{\lambda t}(\lambda > 0)$, where the maximal Lyapunov exponent $\lambda$ of the three-dimensional NS turbulence is mainly determined by the Kolmogorov timescale $\tau$ [1] as $\lambda \propto 1/\tau$. This exponential error growth from the small scales ultimately limits the predictability of large-scale motions [2,3]. Therefore, it is crucial for the prediction of turbulence to reduce such small-scale uncertainty, in other words, to infer small-scale turbulent structures based on observational data from large-scale ones. Recent findings regarding vortex stretching mechanisms, based on the Richardson energy cascade picture [4,5], suggest that this is possible because small-scale vortices are generated by larger-scale ones.

Data assimilation (DA) is suitable for such inferences [6]. Previous studies have determined critical length scales below which turbulent structures can be inferred via DA using only observational data from larger-scale structures [7–14], i.e., the small-scale turbulent dynamics can be reconstructed or synchronized by larger-scale dynamics. Interestingly, in three-dimensional turbulence, a common critical length scale, approximately $20\eta$ where $\eta$ is the Kolmogorov length, has been reported *regardless of the details of the DA algorithms*. This length scale corresponds to a wave number of $k^* \approx 0.2/\eta$, which was found first in the continuous DA [7] and recently found in the four-dimensional variational DA [9] and the nudging DA method [10]. This indicates that the slaving small-scale

dynamics can be understood based on the nature of the Navier-Stokes equations (NSEs) rather than on a specific DA algorithm. As discussed later, this small-scale synchronization is also essential for understanding turbulence physics [4,5] and modeling [15]; however, the physical origins of the critical length scale and the Reynolds-number dependence remain unclear.

In this Letter, we propose a theoretical framework for studying such DA phenomena as a *stability problem*. The proposed framework explains, for the first time, how the critical length scale can be determined by the property of the NSEs. Inspired by the studies of chaos synchronization [16,17], we introduce an invariant manifold, *DA manifold*, in phase space and present a stability analysis, wherein the *transverse* Lyapunov exponents (TLEs) characterize the critical length scale, determining the success or failure of the DA process.

As shown later, the TLEs are related to the maximal Lyapunov exponent (LE) $\lambda$ of the turbulence attractor. In the context of unpredictability in turbulence [2,3], insights into instabilities and the maximal LE in error propagation processes have been elucidated [18–22]. In particular, recent studies discovered that, contrary to the conventional belief, $\lambda\tau$ *increases* with the Reynolds number [18–20]. We show that this novel discovery for the maximal LE provides valuable insights into small-scale synchronization through analysis of the TLEs, and finally conclude that the normalized critical wave number, $k^*\eta$, also increases with the Reynolds number.

The synchronization theory has already been utilized to study DA in chaotic dynamics with noisy observations and model error or mismatch. For instance, pioneering works in

this direction have analyzed the system coupling in DA for the Lorenz-63 model [23] and investigated the spatial structures of synchronization error in DA for the Lorenz-96 model [24]. In this study, we introduce the TLEs to uncover the nature of turbulence governed by the NSEs. In particular, we focus on small-scale synchronization by DA, its dependence on the Reynolds number, and a novel relationship with unpredictability.

*Formulation.*—Following the mathematical formulation by Olson and Titi (2003) [13], we use the continuous DA (CDA). The goal is to reconstruct the velocity field $u$ governed by the NSEs for incompressible flows:

$$\partial_t u + (u \cdot \nabla)u = -\nabla \pi + \nu \Delta u + f, \qquad \nabla \cdot u = 0, \qquad (1)$$

with *unknown* initial conditions $u(0)$ on the $d$-dimensional periodic domain $[0, L]^d$. We refer to $u$ as the *true* velocity field. Here, $\pi$ denotes the pressure, $f$ is the external force, and $\nu$ stands for the kinematic viscosity.

The underlying assumption in CDA is that the true field $u(t)$ can be *partially* observed for any $t \geq 0$. To define this partial observation, we introduce the projections $P_{k_a}$ and $Q_{k_a}$ in the Fourier representation as follows:

$$P_{k_a} v = \sum_{|k| < k_a} \hat{v}_k e^{ik \cdot x}, \qquad Q_{k_a} = I - P_{k_a}, \qquad (2)$$

where $\hat{v}_k$ is the Fourier coefficient of the velocity field $v$ corresponding to the wave number vector $k \in \{2\pi m/L : m \in \mathbb{Z}^d\}$. For each wave number $k_a$, which is a key control parameter in this study, these operators decompose the velocity fields into two parts: large-scale $p := P_{k_a} u$ and small-scale $q := Q_{k_a} u$, i.e., $u = p + q$. The CDA assumes that the large-scale structure of the true velocity field $p(t)$ can be observed at all times $t \geq 0$. Therefore, the primary challenge is reconstructing $q(t)$ under *unknown* initial conditions $q(0)$ using the observational data for $\{p(t)\}_{t \geq 0}$.

To accomplish this, let us consider an approximation $\tilde{u}$ of the true field $u$ decomposed as $\tilde{u} = \tilde{p} + \tilde{q}$, where $\tilde{p} := P_{k_a} \tilde{u}$ and $\tilde{q} := Q_{k_a} \tilde{u}$. As the true data $p$ is available, we set $\tilde{p}(t) \equiv p(t)$, a method called *direct insertion*, i.e., $\tilde{u}(t) = p(t) + \tilde{q}(t)$ for any $t \geq 0$. The evolution equations for $\tilde{q}(t)$ are derived from Eq. (1) using $Q_{k_a}$:

$$\partial_t \tilde{q} + Q_{k_a}(\tilde{u} \cdot \nabla \tilde{u}) = -\nabla \pi' + \nu \Delta \tilde{q} + Q_{k_a} f, \qquad \nabla \cdot \tilde{q} = 0, \quad (3)$$

where $\pi' := Q_{k_a} \tilde{\pi}$ and $\tilde{\pi}$ denotes the pressure corresponding to $\tilde{u}$ [13]. Note that the solution of Eq. (3) is determined by the observational data $\{p(t)\}_{t \geq 0}$ and initial conditions $\tilde{q}(0)$.

In the two-dimensional case $(d = 2)$, Olson and Titi rigorously showed a sufficient condition for successful CDA; for a given kinematic viscosity $\nu$ and forcing term $f$, there exists a critical wave number $k_a^*$ such that, if $k_a > k_a^*$, then $\tilde{q}(t)$ converges to $q(t)$ exponentially, i.e., $\tilde{u}(t) \to u(t)(t \to \infty)$. Therefore, CDA enables us to infer

the small-scale structure of the true velocity field $q$ without the need for direct observation.

In the three-dimensional case $(d = 3)$, Yoshida, Yamaguchi, and Kaneda [7] studied CDA using direct numerical simulations of the NSEs with assimilation at each time step. Starting with the initial velocity fields of $u(t)$ and $\tilde{u}(t)$, the velocity fields $u(t + \Delta t)$ and $\tilde{u}(t + \Delta t)$ were calculated independently using the fourth-order Runge-Kutta method. As an assimilation step, $\tilde{p}(t + \Delta t)$ was replaced by the true state $p(t + \Delta t)$, which results in $\tilde{u}(t + \Delta t) = p(t + \Delta t) + \tilde{q}(t + \Delta t)$. Repeating this procedure, we can conduct numerical experiments of CDA approximately. Applying this method, the critical wave number $k_a^*$ was identified as $k_a^* \eta = 0.2$ in [7].

*Numerical experiments.*—We conducted direct numerical simulations of the three-dimensional NSEs in a periodic box with $L = 2\pi$ driven by a steady force $f(x, y, z) = (-\sin x \cos y, \cos x \sin y, 0)^T$. The Reynolds number used in this work is defined as the temporal average of $\mathrm{Re} = 2E^2/(3\nu\epsilon)$ as [18], where $E$ and $\epsilon$ denote the spatial average of the kinetic energy and energy dissipation rate, respectively. Unless otherwise mentioned, we fix the Reynolds number at $\mathrm{Re} = 570$. Figure 1(a) shows the time series of kinetic energy $E$ in a statistically steady state; see the Supplemental Material [25] about the details of the numerical experiments.

The initial condition of the true system is a turbulent field $u(0) = p(0) + q(0)$ taken from statistically steady states. We obtained the initial condition $\tilde{u}(0)$ by adding a perturbation only to $q(0)$. This procedure is similar to that adopted by Yoshida, Yamaguchi, and Kaneda [7]. Figure 1(b) shows the time series of the approximation error between $u(t)$ and $\tilde{u}(t)$, defined by the energy of the difference field, $\Delta E(t) = 1/2|u - \tilde{u}|^2$, where $|u|^2 = \sum_k |\hat{u}_k|^2$, for three values of $k_a$: $k_a \eta = 0.17$ (solid red), 0.20 (dotted green),
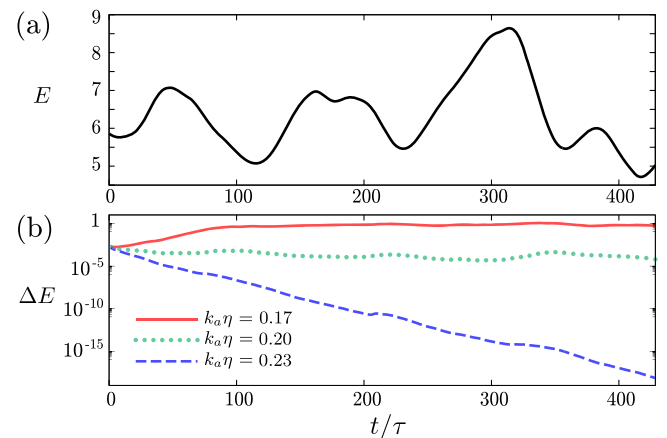


FIG. 1. Continuous data assimilation in the box turbulence. (a) Time series of kinetic energy $E(t)$ in statistically steady states, normalized by the Kolmogorov timescale $\tau$. (b) Time series of approximation error $\Delta E(t)$ between $u(t)$ and $\tilde{u}(t)$ for $k_a \eta = 0.17$ (solid red), 0.20 (dot green), and 0.23 (dashed blue).

and 0.23 (dashed blue). Although the approximation error $\Delta E$ does not decrease for $k_a\eta = 0.17$ and $0.20$, it decreases exponentially for $k_a\eta = 0.23$, thereby indicating a successful DA process. In other words, when $k_a\eta = 0.23$, small-scale structures of the velocity field, $\boldsymbol{q}$, can be determined by the sequential data of large-scale structures, $\boldsymbol{p}$. This result is quantitatively the same as that of the previous studies [7–10]; i.e., the critical wave number is $k_a^*\eta = 0.2$ irrespective of the differences in the forcing term and details of the DA methods. For the spatiotemporal dynamics of vortex structures reconstructed using the DA process, refer to the movie provided as part of the Supplemental Material [25].

*DA manifold and its stability.*—To understand the experimental results of the DA, we study the (skew-product) dynamical system $(\boldsymbol{p},\boldsymbol{q},\tilde{\boldsymbol{q}})$ determined by the NSEs, which can be expressed as $\partial_t\boldsymbol{p} = \boldsymbol{F}(\boldsymbol{p},\boldsymbol{q})$, $\partial_t\boldsymbol{q} = \boldsymbol{G}(\boldsymbol{p},\boldsymbol{q})$ (base system), and Eq. (3), $\partial_t\tilde{\boldsymbol{q}} = \boldsymbol{G}(\boldsymbol{p},\tilde{\boldsymbol{q}})$ (fiber system). Inspired by the studies of chaos synchronization [16,17], we focus on the manifold defined by $\mathcal{M} = \{(\boldsymbol{p},\boldsymbol{q},\tilde{\boldsymbol{q}}):\tilde{\boldsymbol{q}} = \boldsymbol{q}\}$, which is invariant because any solution trajectory starting from an initial point on $\mathcal{M}$ remains within it. To emphasize its importance within the context of DA, we refer to $\mathcal{M}$ as the *DA manifold*, which corresponds to the synchronization manifold in synchronization theory. The inset of Fig. 2 shows schematics of the solution trajectory and $\mathcal{M}$ in the phase space.

The success of the DA process implies asymptotic stability of $\mathcal{M}$. Let us now consider a successful DA process, i.e., a solution trajectory starting at an initial point apart from $\mathcal{M}$, i.e., $\boldsymbol{q}(0) \neq \tilde{\boldsymbol{q}}(0)$, converges to $\mathcal{M}$
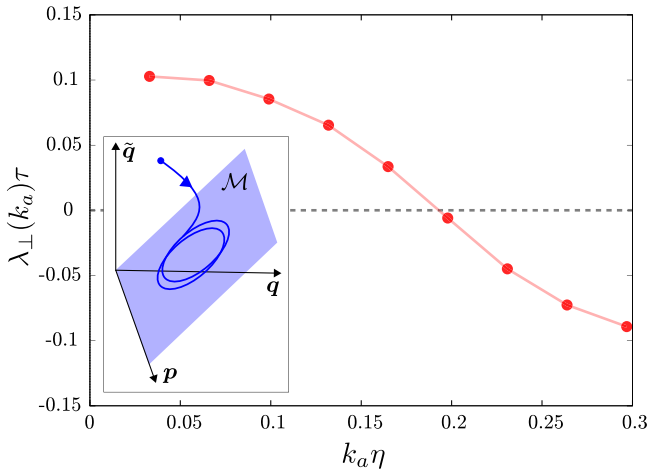


FIG. 2. Transverse Lyapunov exponents (TLEs) $\lambda_\perp(k_a)$ as a function of the wave number $k_a$ normalized by the Kolmogorov time $\tau$ and length $\eta$. The sign changes from positive to negative at $k_a\eta \simeq 0.2$, characterizing the success or failure of the DA process shown in Fig. 1(b). The inset shows a schematic of the phase space and DA manifold $\mathcal{M}$, illustrating the successful DA process, where the solution trajectory from the initial point (the blue dot) approaches $\mathcal{M}$.

asymptotically in time; that is, $\tilde{\boldsymbol{q}}(t) \to \boldsymbol{q}(t)\,(t \to +\infty)$, as illustrated in the inset of Fig. 2. This can be interpreted as $\mathcal{M}$ being asymptotically stable. The linear stability analysis of $\mathcal{M}$ gives *a priori* knowledge on whether the DA process succeeds or fails. To study the stability, we introduce an infinitesimal perturbation to the velocity field $\delta\boldsymbol{q} = \tilde{\boldsymbol{q}} - \boldsymbol{q}(\neq \boldsymbol{0})$ and derive the following variational equations:

$$\partial_t\delta\boldsymbol{q} + Q_{k_a}(\boldsymbol{u}\cdot\nabla\delta\boldsymbol{q}) + Q_{k_a}(\delta\boldsymbol{q}\cdot\nabla\boldsymbol{u}) = -\nabla\delta\pi + \nu\Delta\delta\boldsymbol{q}, \quad (4)$$

where $\delta\pi = \pi_2' - \pi_1'$ is the perturbation in the pressure field (see its derivation in the Supplemental Material [25]). The transverse Lyapunov exponent (TLE) is defined as

$$\lambda_\perp(k_a) := \lim_{T\to\infty}\frac{1}{T}\ln|\delta\boldsymbol{q}(T)|, \quad (5)$$

if the limit exists. A negative TLE, $\lambda_\perp < 0$, indicates asymptotic linear stability of the DA manifold $\mathcal{M}$, which implies a successful DA process. By contrast, if the TLE is positive, $\lambda_\perp > 0$, the DA manifold $\mathcal{M}$ is linearly unstable, which implies a failure of the DA process. The TLE is an ergodic quantity of the turbulent attractor, which characterizes the average exponential growth or decay rate of the norm of the perturbation along the solution trajectory within $\mathcal{M}$.

The TLEs $\lambda_\perp(k_a)$ explain the results of the numerical experiments for the CDA in the NS turbulence shown in Fig. 1(b). The numerical integration of the variational equations (4) coupled with the NSEs (1) for $\boldsymbol{u}$ gives a TLE $\lambda_\perp(k_a)$ for each fixed $k_a$. Figure 2 shows the normalized TLE $\lambda_\perp(k_a)\tau$ as a function of the normalized wave number, $k_a\eta$ (refer to the Supplemental Material [25] for details on the numerical methods and the convergence of the TLEs). For $k_a\eta < 0.2$, the TLEs are positive, $\lambda_\perp > 0$; that is, the DA manifold $\mathcal{M}$ is unstable. The TLE decreases as $k_a$ increases and becomes negative for $k_a\eta > 0.2$; that is, $\mathcal{M}$ is stable. The change in stability of $\mathcal{M}$ at the critical wave number $k_a^* \simeq 0.2/\eta$ explains the results of the success or failure of the DA process shown in previous studies [7,8,10] and Fig. 1(b).

*Reynolds-number dependence.*—To study the Reynolds number dependence, the normalized TLEs $\lambda_\perp\tau$ for Re = 1400 are shown as blue open circles in Fig. 3. For reference, the red circles denote the TLEs $\lambda_\perp(k_a)\tau$ for Re = 570, which are the same as those in Fig. 2. The critical wave number $k_a^*\eta$, defined by the change in the sign of the TLEs, increases with Re; $k_a^*\eta$ is higher for Re = 1400 than for Re = 570. To understand this Re dependence of the critical wave number, we consider the asymptotic forms of the TLE $\lambda_\perp(k_a)$ for both low and high wave numbers $k_a$.

In the low-wave number limit, the TLE is reduced to the maximal LE of the turbulent attractor. The variational equations (4) describe the perturbation lying in the wave number subspace higher than $k_a$ since there is no uncertainty in the wave number subspace lower than $k_a$. As $k_a$
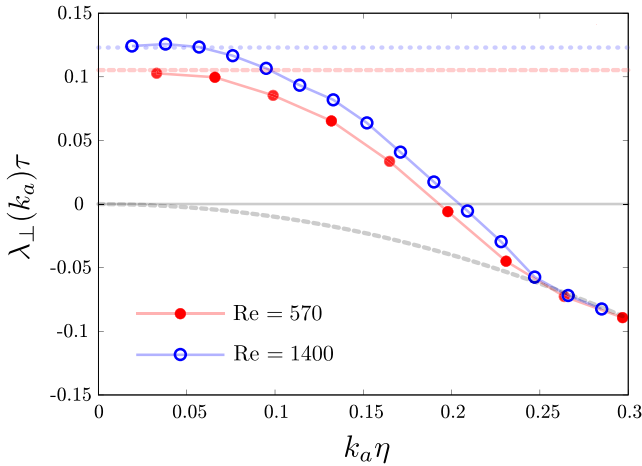
FIG. 3. Reynolds-number dependence of TLEs. The normalization is the same as in Fig. 2. The red solid and blue open circles represent the normalized TLEs for Re = 570 and Re = 1400, respectively. The horizontal red dashed and blue dotted lines indicate the values of the normalized maximal LEs $\lambda\tau$ for Re = 570 and Re = 1400, respectively. The gray dashed curve corresponds to $\lambda_\perp(k_a)\tau = -(k_a\eta)^2$, where the viscous term determines the perturbation dynamics.

decreases, the perturbation dynamics become less confined. At $k_a = 0$, the perturbation can evolve in the whole wave number space; that is, there is no confinement. In this case, $Q_{k_a} = I$ (the identity operator), and the variational equations (4) are reduced to the standard variational equations of the NSEs, under which the TLE reduces to the maximal LE of the turbulent attractor, that is $\lambda_\perp(0) = \lambda$.

The horizontal red dashed and blue dotted lines in Fig. 3 show the values of the maximal LEs $\lambda\tau$ for Re = 570 and Re = 1400, respectively. The TLEs for each Re number converge to the normalized LEs as $k_a\eta \to +0$. For Re = 570, the maximal LE is $\lambda\tau \simeq 0.11$, and it increases with Re. These results agree with the recent findings [18–20] claiming that the maximal LE increases with Re faster than predicted by dimensional analysis, that is, $\lambda \propto 1/\tau$. In particular, the lower inset of Fig. 4 of Boffetta and Musacchio [18] shows that $\lambda\tau$ is an increasing function of Re, which is contrary to the conventional belief.

In the high-wave number limit of $\lambda_\perp(k_a)$, the perturbation is confined to the higher-wave number region where the viscous term is dominant and $\partial_t \delta q \sim \nu\Delta\delta q$. This suggests that $\lambda_\perp(k_a)\tau = -(k_a\eta)^2$, as denoted by the gray dashed curve in Fig. 3. The TLEs for different Reynolds numbers collapse onto this curve in the high-wave number region.

In summary, the TLEs $\lambda_\perp(k_a)$ shown in Fig. 3 connect the maximal LEs $\lambda$ at $k_a = 0$ with the curve $-(k_a\eta)^2$ for the high $k_a$. In addition, the maximal LE, $\lambda_\perp(0) = \lambda$, increases with Re [18–20]. These findings indicate that an upward shift of the graph $\lambda_\perp(k_a)\tau$ with increasing Re leads to an increase in the critical wave number $k_a^*$.

*Discussion and conclusion.*—DA is becoming an increasingly significant tool in data-driven forecasting. However, little is known about the critical wave number $k^*$, which plays a key role in various DA methods for three-dimensional turbulence [7,8,10–12]. This study establishes a novel framework based on the chaos synchronization theory [16,17], and it clarifies the critical wave number based on the TLEs, which are the ergodic quantities of the NSEs. Furthermore, considering the novel discovery of the Reynolds number dependence of the maximal LE [18–20], the relationship between the TLEs and the maximal LE suggests that the critical wave number increases with Re.

Further study of the Reynolds number dependence of $k_a^*\eta$ is particularly interesting. Recent findings [18–20] suggest that $\lambda_\perp(0)\tau(= \lambda\tau)$ increases unboundedly with Re. The critical wave number, $k_a^*\eta$, normalized by the mean Kolmogorov scale $\eta$ is expected to also increase unboundedly with Re. Solving this problem requires both a large-scale computation of TLEs over a wide range of Reynolds numbers and consideration of the spatiotemporal intermittency beyond the standard Kolmogorov scaling argument, which may be related to the singularity of the NSEs as argued in [8].

Besides the phase-space dynamics studied in this Letter, understanding the turbulent dynamics in the *physical* space is also complementarily necessary. Remarkably, the critical wave number, $k^* = 0.2/\eta$, has been identified in a context unrelated to DA. Specifically, it was discovered in a recent study of vortex stretching, which revealed a far dissipation range for wave numbers exceeding $k^*$, i.e., for $k > k^*$ [5]. In terms of the Kolmogorov-Richardson energy cascade, the turbulent dynamics in the far dissipation range terminate the cascade process. Although structures in the range acquire the energy from larger scales, they cannot transfer it to smaller ones but dissipate it there instead. This may imply that they are slaving, or "synchronizing," to larger-scale structures and gives an interpretation of the small-scale slaving dynamics in the DA context.

In addition to this insight, a key to the complete understanding of the slaving small-scale dynamics will be found in the physical space structure of the covariant Lyapunov vectors (CLVs) [26–30] corresponding to the LEs; these are "unstable modes" of turbulent structures, such as the hierarchy of antiparallel vortex tubes [4,5]. When $\lambda_\perp < 0$, the variable $q$ is uniquely determined by $p$; in such a case, if we represent $q = \phi(p)$, the graph, $\mathcal{G}[\phi] = \{u : u = p + \phi(p)\}$, may correspond to the *inertial manifold* [31,32] of the three-dimensional NSEs. TLE will be one of the fundamental tools for analyzing high-dimensional chaotic dynamical systems with hierarchical spatiotemporal scales; therefore, it is crucial, from a viewpoint of mathematical physics, to provide rigorous proofs for the existence of the TLE $\lambda_\perp(k_a)$ and its smooth variation with $k_a$, as an extension of the Oseledets theorem.

The small-scale dynamics and synchronization can relate to the key concepts in turbulence research, such as unpredictability, energy cascade, intermittency, singularity, and inertial manifold. Furthermore, future studies based on our DA approach to small-scale turbulence may also influence data-driven methods [15,33–35]. For example, while this Letter focuses on linear stability characterized by the TLEs, *nonlinear* stability of the DA manifold $\mathcal{M}$ can be useful for DA research, such as superexponential convergence of nonlinear CDA algorithm for the two-dimensional NSEs [36]. Disentangling the above relationships based on our theoretical framework will provide new insights into the NS turbulence, leading to novel data-driven methods, including DA algorithms.

---

*inubushi@rs.tus.ac.jp

[1] D. Ruelle, Microscopic fluctuations and turbulence, Phys. Lett. **72A**, 81 (1979).

[2] E. N. Lorenz, The predictability of a flow which possesses many scales of motion, Tellus **21**, 289 (1969).

[3] C. E. Leith and R. H. Kraichnan, Predictability of turbulent flows, J. Atmos. Sci. **29**, 6 (1972).

[4] S. Goto, Y. Saito, and G. Kawahara, Hierarchy of anti-parallel vortex tubes in spatially periodic turbulence at high Reynolds numbers, Phys. Rev. Fluids **2**, 064603 (2017).

[5] T. Yoneda, S. Goto, and T. Turuhashi, Mathematical reformulation of the Kolmogorov–Richardson energy cascade in terms of vortex stretching, Nonlinearity **35**, 1380 (2022).

[6] S. Reich and C. Cotter, *Probabilistic Forecasting and Bayesian Data Assimilation* (Cambridge University Press, Cambridge, England, 2015).

[7] K. Yoshida, J. Yamaguchi, and Y. Kaneda, Regeneration of small eddies by data assimilation in turbulence, Phys. Rev. Lett. **94**, 014501 (2005).

[8] C. C. Lalescu, C. Meneveau, and G. L. Eyink, Synchronization of chaos in fully developed turbulence, Phys. Rev. Lett. **110**, 084102 (2013).

[9] Y. Li, J. Zhang, G. Dong, and N. S. Abdullah, Small-scale reconstruction in three-dimensional Kolmogorov flows using four-dimensional variational data assimilation, J. Fluid Mech. **885**, A9 (2020).

[10] P. C. D. Leoni, A. Mazzino, and L. Biferale, Synchronization to big data: Nudging the Navier–Stokes equations for data assimilation of turbulent flows, Phys. Rev. X **10**, 011023 (2020).

[11] A. Vela-Martín, The synchronisation of intense vorticity in isotropic turbulence, J. Fluid Mech. **913**, R8 (2021).

[12] M. Wang and T. A. Zaki, Synchronization of turbulence in channel flow, J. Fluid Mech. **943**, A4 (2022).

[13] E. Olson and E. S. Titi, Determining modes for continuous data assimilation in 2D turbulence, J. Stat. Phys. **113**, 799 (2003).

[14] M.-A. Nikolaidis and P. J. Ioannou, Synchronization of low Reynolds number plane Couette turbulence, J. Fluid Mech. **933**, A5 (2022).

[15] S. Matsumoto, M. Inubushi, and S. Goto (to be published).

[16] T. Yamada and H. Fujisaka, Stability theory of synchronized motion in coupled-oscillator systems. II: The mapping approach, Prog. Theor. Phys. **70**, 1240, 32 (1983).

[17] E. Ott and J. C. Sommerer, Blowout bifurcations: The occurrence of riddled basins and on-off intermittency, Phys. Lett. A **188**, 39 (1994).

[18] G. Boffetta and S. Musacchio, Chaos and predictability of homogeneous-isotropic turbulence, Phys. Rev. Lett. **119**, 054102 (2017).

[19] P. Mohan, N. Fitzsimmons, and R. D. Moser, Scaling of Lyapunov exponents in homogeneous isotropic turbulence, Phys. Rev. Fluids **2**, 114606 (2017).

[20] B. Arjun and R. D. J. G. Ho, Chaotic properties of a turbulent isotropic fluid, Phys. Rev. Lett. **120**, 024101 (2018).

[21] N. B. Budanur and H. Kantz, Scale-dependent error growth in Navier-Stokes simulations, Phys. Rev. E **106**, 045102 (2022).

[22] P. V. Kashyap, Y. Duguet, and O. Dauchot, Linear instability of turbulent channel Flow, Phys. Rev. Lett. **129**, 244501 (2022).

[23] S. C. Yang, D. Baker, H. Li, K. Cordes, M. Huff, G. Nagpal, E. Okereke, J. Villafane, E. Kalnay, and G. S. Duane, Data assimilation as synchronization of truth and model: Experiments with the three-variable Lorenz system, J. Atmos. Sci., **63**, 2340 (2006).

[24] I. G. Szendro, M. A. Rodríguez, and J. M. López, On the problem of data assimilation by means of synchronization, J. Geophys. Res. **114**, D20109 (2009).

[25] See Supplemental Material at http://link.aps.org/supplemental/10.1103/PhysRevLett.131.254001 for the details of the numerical experiments and the theoretical framework.

[26] S. Kida and K. Ohkitani, Spatiotemporal intermittency and instability of a forced turbulence, Phys. Fluids **4**, 1018 (1992).

[27] F. Ginelli, P. Poggi, A. Turchi, H. Chaté, R. Livi, and A. Politi, Characterizing dynamics with covariant Lyapunov vectors, Phys. Rev. Lett. **99**, 130601 (2007).

[28] M. Inubushi, Miki U. Kobayashi, S. Takehiro, and M. Yamada, Covariant Lyapunov analysis of chaotic Kolmogorov flows, Phys. Rev. E **85**, 016331 (2012).

[29] M. Inubushi, S. Takehiro, and M. Yamada, Regeneration cycle and the covariant Lyapunov vectors in a minimal wall turbulence, Phys. Rev. E **92**, 023022 (2015).

[30] Y. Chen, A. Carrassi, and V. Lucarini, Inferring the instability of a dynamical system from the skill of data assimilation exercises, Nonlinear Processes Geophys. **28**, 633 (2021).

[31] H. Yang, K. A. Takeuchi, F. Ginelli, H. Chaté, and G. Radons, Hyperbolicity and the effective dimension of spatially extended dissipative systems, Phys. Rev. Lett. **102**, 074102 (2009).

[32] James C. Robinson, *Infinite-Dimensional Dynamical Systems: An Introduction to Dissipative Parabolic PDEs and the Theory of Global Attractors*, Cambridge Texts in Applied Mathematics, Series Number 28, (Cambridge University Press, Cambridge, England, 2001).

[33] A. Mashayek, N. Reynard, F. Zhai, K. Srinivasan, A. Jelley, A. N. Garabato, and C. P. Caulfield, Deep ocean learning of small scale turbulence, Geophys. Res. Lett. **49**, 15 (2022).

[34] M. Inubushi and S. Goto, Transfer learning for nonlinear dynamics and its application to fluid turbulence, Phys. Rev. E **102**, 043301 (2020).

[35] M. Konishi, M. Inubushi, and S. Goto, Fluid mixing optimization with reinforcement learning, Sci. Rep. **12**, 14268 (2022).

[36] E. Carlson, A. Larios, and E. S. Titi, Super-exponential convergence rate of a nonlinear continuous data assimilation algorithm: The 2D Navier–Stokes equations paradigm, arXiv:2304.01128.